

# DNA-Encircled Lipid Bilayers

*Katarina Iric<sup>1,3</sup>, Madhumalar Subramanian<sup>2,3</sup>, Jana Oertel<sup>3</sup>, Nayan P. Agarwal<sup>1</sup>, Michael  
Matthies<sup>1</sup>, Xavier Periole<sup>4</sup>, Thomas P. Sakmar<sup>5</sup>, Thomas Huber<sup>5</sup>, Karim Fahmy<sup>2,3\*</sup>, and  
Thorsten-Lars Schmidt<sup>1,6,7\*</sup>*

1 Center for Advancing Electronics Dresden (cfaed), Technische Universität Dresden  
01062 Dresden, Germany

2 Biotechnology Center, Tatzberg 47-49, Technische Universität Dresden, 01307 Dresden,  
Germany

3 Helmholtz-Zentrum Dresden-Rossendorf, Institute of Resource Ecology  
Bautzner Landstrasse 400, 01328 Dresden, Germany

4 Department of Chemistry, Aarhus University, Aarhus C, Denmark

5 Laboratory of Chemical Biology & Signal Transduction, Rockefeller University  
1230 York Avenue, NY 10065 New York, USA

6 B CUBE - Center for Molecular Bioengineering, Technische Universität Dresden, 01062  
Dresden, Germany

7 Chemistry and Food Chemistry, Technische Universität Dresden, 01062 Dresden, Germany

**KEYWORDS:** DNA Nanotechnology, membrane mimetics, lipid bilayers, MD simulations

**ABSTRACT:** Lipid bilayers and lipid-associated proteins play a crucial role in biology. As *in vivo* studies and manipulation are inherently difficult, several membrane-mimetic systems have been developed to enable investigation of lipidic phases, lipid-protein interactions, membrane protein function and membrane structure *in vitro*. Controlling the size and shape, or site-specific functionalization is, however, difficult to achieve with established membrane mimetics based on membrane scaffolding proteins, polymers or peptides. In this work, we describe a route to leverage the unique programmability of DNA nanotechnology and create DNA-encircled bilayers (DEBs), which are made of multiple copies of an alkylated oligonucleotide hybridized to a single-stranded minicircle. To stabilize the hydrophobic rim of the lipid bilayer, and to prevent formation of lipid vesicles, we introduced up to 2 alkyl chains per helical that point to the inside of the toroidal DNA ring and interact with the hydrophobic side chains of the encapsulated lipid bilayer. The DEB approach described herein provides unprecedented control of size, and allows the orthogonal functionalizations and arrangement of engineered membrane nanoparticles and will become a valuable tool for biophysical investigation of lipid phases and lipid-associated proteins and complexes including structure determination of membrane proteins and pharmacological screenings of membrane proteins.

Cell compartmentalization by membranes is crucial in biology and membrane-associated proteins contribute to fundamental cellular processes in energy conversion, cell communication and signal transduction. Membrane protein function is often linked to conformational transitions which may be critically affected by lipid protein interactions.<sup>1-5</sup> As *in vivo* investigations are often very challenging, such functional implications of lipid protein interactions<sup>6</sup> can be more easily studied *in vitro* with artificial membrane-mimetic systems which provide a native-like lipid environment. For example, planar discoidal nanoscale lipid bilayers surrounded by amphipathic polymers<sup>7</sup> or surfactant-like helical peptides<sup>8</sup> have been described. Discoidal planar bilayers are mostly assembled from dimeric apolipoprotein AI-derived proteins, which encircle a lipid bilayer, thereby sealing its hydrophobic rim. These membrane scaffolding proteins (MSPs) have been produced from different sources and typically support lipid bilayers of 10-16 nm in diameter.<sup>9-11</sup> The resulting lipid-protein nanodiscs (NDs) may contain a single membrane protein or two proteins.<sup>12</sup> However, apolipoprotein-based systems exhibit high structural flexibility<sup>13</sup>, which has restricted their use for high resolution structure determination of reconstituted membrane proteins. Recent efforts employ circularization of MSPs to overcome some of these limitations.<sup>14</sup> Nonetheless, controlling the diameter, stability or site-specifically introducing functional elements or orthogonal interaction elements remains very challenging or laborious for all of the established membrane mimetic systems.

In contrast, DNA nanotechnology allows generation of arbitrarily shaped structures with Å precision by a bottom-up self-assembly process.<sup>15</sup> For large, megadalton-sized structures typically measuring tens to hundreds of nanometers, the DNA origami approach became particularly popular due to its robustness and versatility.<sup>16-18</sup> For some applications, smaller structures such as tetrahedra,<sup>19</sup> icosahedra,<sup>20</sup> or structures from DNA minicircles (MCs).<sup>21-25</sup> consisting of fewer

synthetic oligonucleotides can be better suited and are more economical. Furthermore, DNA structures can be functionalized with a large variety of artificial elements including small molecules, fluorophores, functional groups, biomolecules or inorganic nanoparticles<sup>26</sup> in a modular and programmable fashion.<sup>18</sup> To enable interactions between negatively charged hydrophilic DNA and lipids, several oligonucleotide modifications have been previously employed including cholesterol, porphyrin or phospholipid modifications.<sup>27</sup> In this way, DNA based membrane penetrating pores were created,<sup>28</sup> DNA Origami structures were anchored to the surface of liposomes.<sup>29</sup> Furthermore, liposomes can be wrapped around DNA origami structures creating an envelope virus mimic,<sup>30</sup> or liposomes can be grown inside of DNA structures,<sup>31</sup> even with controllable shapes.<sup>32</sup> Due to the tendency of lipids to form liposomes, it is, however, challenging to create finite, planar lipid bilayers and no nanoscale lipid bilayers stabilized by DNA were shown to date where both sides of the membrane are accessible and can be essential when studying transmembrane complexes.

With the aim of enabling a level of programmability not achievable with the present membrane-mimetics, we report the protein-independent oligonucleotide-based formation of planar, nanoscale, discoidal lipid bilayers. In our design, we conceptually replace the MSP of “nanodiscs” by a site-specifically alkylated circular dsDNA scaffold with similar design and synthesis approaches as demonstrated earlier.<sup>21–25</sup> For this, a double-stranded MC (dsMC) with 147 base pairs (bp) is composed of a circularized 147 nucleotide (nt) long oligonucleotide hybridized to seven identical copies of a short oligonucleotide (21 nt each). With a thickness of 2 nm and a rise of 0.335 nm/bp for dsDNA, their outer diameter is expected to be 16.7 nm and the inner diameter 14.7 nm.

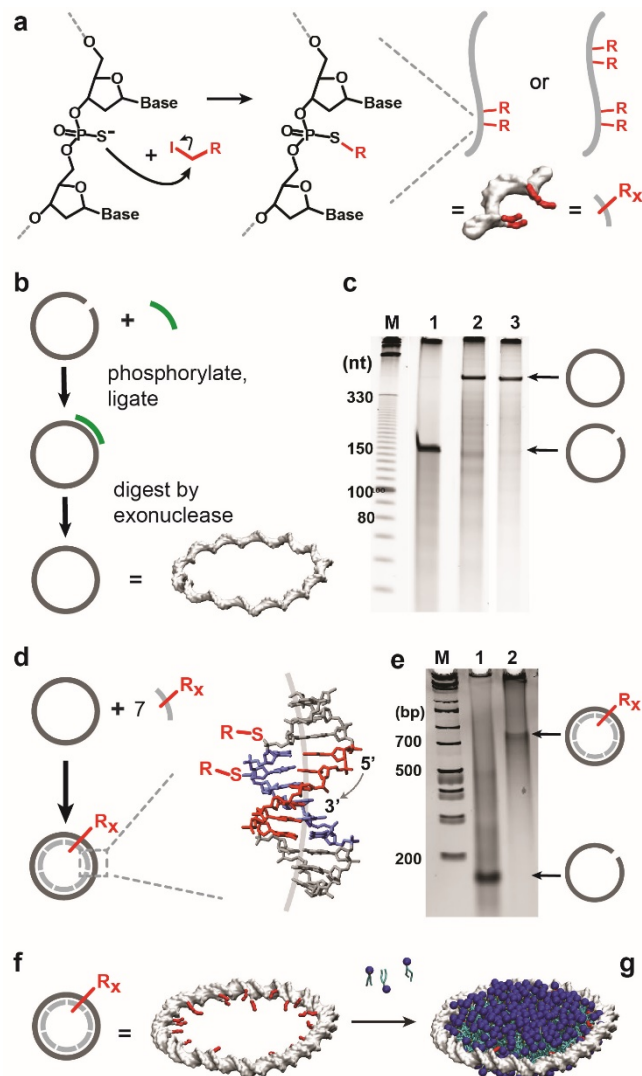


**Figure 1.** Synthesis of DEBs. a) Short oligonucleotides with two or four phosphorothioates are alkylated with alkyl-iodides (red). b) A circular single-stranded template is synthesized by enzymatic splint ligation from a long, linear oligonucleotide (grey). Residual splints (green) and linear templates are digested by exonuclease treatment. c) A denaturing PAGE gel confirms the synthesis of the single-stranded minicircle (ssMC). M, molecular size marker (nt); lane 1, linear long oligonucleotide; lane 2, ligation reaction before exonuclease treatment; lane 3, exonuclease

digest. d) The ssMC is hybridized with seven alkylated oligonucleotides into double-stranded MCs (dsMC). The position of alkylations, and the intrinsic curvature of the A-tracts (grey line in the center of the helix, exaggerated) in a model of an A-tract<sup>33,34</sup> (adapted from PDB structure 1FZX). Adenosines are coloured red, thymidines blue. e) native PAGE gel. M, marker (base pairs); 1, linear long oligonucleotide; 2, the assembled dsMC complex. f) The dsMC is incubated with phospholipids (blue) to form a mature DEB (g).

To achieve highest cost-effectiveness and scalability of a linker-free chemical modification even in the middle of an oligonucleotide, we alkylated phosphorothioates with alkanyl (alkyl) iodides (Figure 1 a).<sup>35</sup> Commercially prepared oligonucleotides containing two or four internal phosphorothioates were reacted with an excess of ethyl iodide, butyl iodide or decyl iodide. The respective products were HPLC purified and alkylation confirmed by ESI mass spectrometry (experimental details and procedures in Supporting Information).

To define the inside and outside of the desired toroidal dsMC, the sequence was designed with 14 intrinsically curved A-tracts,<sup>33,36</sup> as depicted in Figure 1 d.<sup>34</sup> First, a single-stranded minicircle (ssMC) was prepared from one long oligonucleotide (147 nt) by enzymatic splint ligation (Figure 1 b). Residual linear long oligonucleotides, splints and linear side products were enzymatically removed by a treatment with exonuclease I/III (Figure 1 b-c). Next, the ssMCs were hybridized with the alkylated oligonucleotides by slow cooling. Excess oligonucleotides were removed by ultrafiltration and the double-stranded minicircles (dsMCs) analyzed by native agarose gel electrophoresis (Figure 1 e), atomic force microscopy (AFM) and transmission scanning electron microscopy (tSEM).

Finally, the alkylated dsMCs were filled with a lipid bilayer (Figure 1 f-g). Similar to ND formation with MSPs, removal of detergent from a detergent-solubilized mix of the alkylated dsMCs and stoichiometric amounts of phospholipids (MC:lipid was 1:450) led to the self-assembly of the components into nanoscale discoidal particles (Figure 2).

AFM imaging of the dsMCs and DEBs revealed a doubling of the height due to the addition of the lipid bilayer (Figure 2 a-c). The tSEM images (Figure 2 d, f) also confirm the presence of a lipid bilayer in the DEBs. Short (14 ethyl) and longer alkyl chains (28 decyl), produced DEBs (Figure 2 e,f), but DEBs with longer alkyl chains formed with higher yields (Figure 3 a-c).

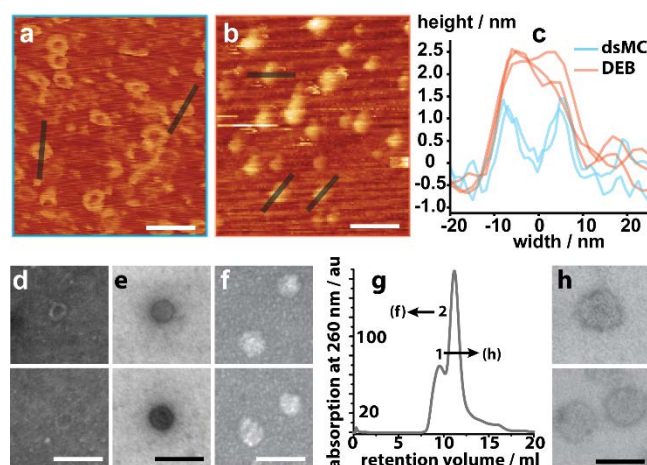


**Figure 2.** Analysis of dsMCs and DEBs. a) an AFM image of empty dsMCs (R = 4 butyl) and corresponding DEBs (b). c) height profiles. d) tSEM images of empty dsMCs. e) tSEM image of a DEB with 14 ethyl modifications (positively stained). f) tSEM image of a DEB with 28 decyl modifications. g) elution profile of a size exclusion chromatography (SEC) run of a DEB preparation. Fraction 1 contains dimeric DEBs (h), fraction 2 monomers (f). Scale bars, 50 nm.



DEBs were purified either by size exclusion chromatography (Figure 2 g) or ultracentrifugation, where DEBs formed one sharp band which contained both lipids and DNA. In syntheses of ssMCs at high concentrations, dimeric ligation products occurred as a side product (Figure S1). They were separated by SEC from the monomers and exhibited twice the circumference of monomers (Figure 2 g,h). This result shows that DEBs can be prepared with a wide range of controllable sizes.

Next, we compared the thermotropic phase transition of DMPC in conventional MSP-based NDs with that of DEBs by using the emission of the lipophilic dye LAURDAN as a sensor of lipid order.<sup>37</sup> The midpoint temperature  $T_m$  for the gel to liquid transition of DMPC in DEBs was 25 °C and agrees with literature data on DMPC vesicles,<sup>38</sup> whereas DMPC in NDs showed a slightly higher  $T_m$  (31 °C) as reported.<sup>39</sup> However, the change of the generalized polarization (GP) value in DEBs was only ~50 % of that in NDs transition, which may indicate restricted lipid mobility at the alkylated DNA-lipid interface. Upon doping of the DMPC bilayer with the cationic lipid DMTAP, no phase transition was observed (Figure S2), which we attribute to the additional electrostatic interactions of the positively charged head groups with the dsMC, and to a preferential binding of LAURDAN at the DNA lipid interface (Supporting Information).

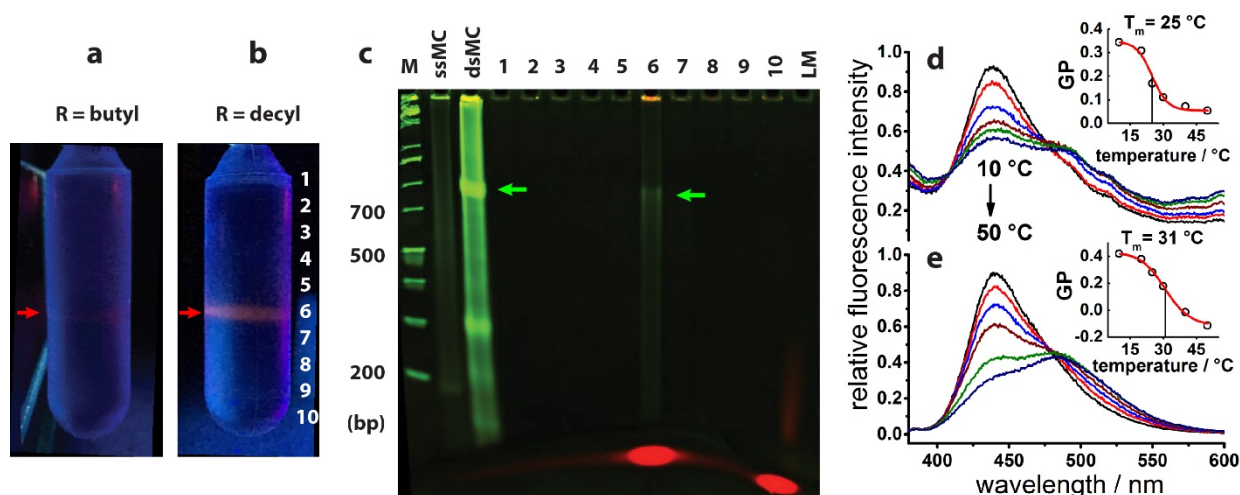


**Figure 3:** Analysis of DEBs. Gradient ultracentrifugation results of Rhodamine-PE- containing DEBs with 28 butyl groups (a), and 28 decyl groups (b) that were analyzed by native SDS PAGE (c). LM = control lipid mix. d-e) Lipid phase transition of DEBs. Emission spectra of LAURDAN ( $\lambda_{\text{exc}} = 340 \text{ nm}$ ) in DMPC-filled DEBs carrying two ethyl groups per hybridized 21-mer (d) and in MSP-based NDs (e) recorded at 10 °C, 20 °C, 25 °C, 30 °C, 40 °C and 50 °C. Inserts show the temperature dependence of the generalized polarization,  $GP = (I_{440} - I_{490}) / (I_{440} + I_{490})$  which reveals the gel to liquid phase transition<sup>41</sup> ( $T_m$ : transition midpoint temperature).

We next prepared a coarse grain molecular dynamics (CGMD) simulation of a DEB using the MARTINI force field (Figure 4).<sup>40,41</sup> In agreement with experimental results, a DEB was stable over a 5 microsecond duration with the 4 nm thick DMPC bilayer encircled by the 2 nm thick dsDNA rim. The interaction of the alkyl chains (Figure 4a-b, red) with the lipid bilayer could also be clearly observed.

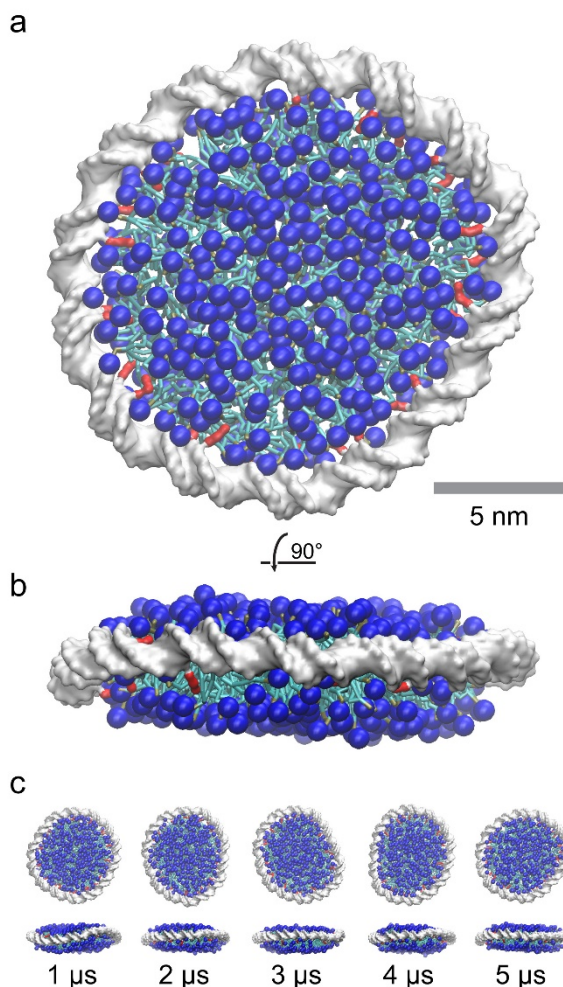


**Figure 4.** Coarse grain molecular dynamics model of a DEB composed of a 147 bp dsMC with 28 dodecyl groups and 434 DMPC lipids. DNA is white, alkyl chains red, DMPC head groups blue. a) View down the membrane normal of a structure at the end of the 5 microseconds long trajectory. b) rotated 90 degrees. c) Snapshots after 1-microsecond intervals.

In summary, we report DEBs as a novel strategy to prepare nanoscale discoidal bilayer structures encapsulated by an alkylated dsMC DNA. With the DEB technology we realize for the first time the use of DNA in order to shape planar, non-spherical, lipid bilayers while providing access to

both sides of the bilayer. In contrast to the DNA origami approach, requiring hundreds of oligonucleotides and expensive single-stranded scaffold strands, the minimalistic DEB design requires only two synthetic oligonucleotides, which facilitates upscaling. Moreover, only one oligonucleotide has to be chemically modified, and the chosen alkylation of phosphorothioate is among the most economical and scalable modification approaches. With our design, we achieved a high alkylation density of up to two alkylations per helical turn without an additional linker directly on the backbone of the DNA minicircle, to stabilize the rim of the lipid bilayer in an aqueous environment in a highly defined fashion. We anticipate that the extensive repertoire available in DNA nanotechnology will allow to further control the size and shape of DEBs and facilitate their site-specific modification. This way, higher order supramolecular assemblies and surface attachment of the DEBs can be readily achieved by DNA hybridization approaches rather than using chemical modification required with MSPs. Furthermore, DEBs hold great promise for the incorporation of membrane proteins, opening new routes for biophysical and structural studies of membrane proteins in their native lipid environment including structure determination by XFEL (X-ray free electron laser) or cryo EM as well as for pharmacological screenings.

## ASSOCIATED CONTENT

**Supporting Information.** The following files are available free of charge.

Supporting information (PDF) containing materials and methods, and Supporting Figures.

## AUTHOR INFORMATION

### Corresponding Author

\* E-mail: [Thorsten-Lars.Schmidt@tu-dresden.de](mailto:Thorsten-Lars.Schmidt@tu-dresden.de). Tel/ Fax: +49-351-653-36487.

\* E-mail: [K.Fahmy@HZDR.de](mailto:K.Fahmy@HZDR.de). Tel: +49-351-260-2952. Fax: +49-351-260-13233.

## **Funding Sources**

This work was funded by the DFG through a starting grant of cfaed to T.L.S, a stipend of the DIGS-BB to K.I. and a networking grant from the Helmholtz-Association to K.F. and M.S. Support was also provided to T.H. from the Robertson Therapeutic Development Fund.

## **Notes**

K.F, KI and T.L.S. have filed a provisional patent application.

## **ACKNOWLEDGMENT**

We thank Prof. Zhang and Dr. Reddavid (B CUBE) for help with HPLC-ESI MS. We are grateful to Lisa Nucke and Michael Matthies for many helpful discussions and to Jenny Philipp for technical support. We acknowledge the use of the imaging facilities in the Dresden Center for Nanoanalysis (DCN), the skillful advice from Dr. Löffler and the use of the AFM of Prof. Mertig (TU Dresden).

## REFERENCES

- (1) Cymer, F.; von Heijne, G.; White, S. H. *J. Mol. Biol.* **2015**, *427* (5), 999–1022.
- (2) Sandoval, A.; Eichler, S.; Madathil, S.; Reeves, P. J.; Fahmy, K.; Böckmann, R. A. *Biophys. J.* **2016**, *111* (1), 79–89.
- (3) Fischermeier, E.; Pospíšil, P.; Sayed, A.; Hof, M.; Solioz, M.; Fahmy, K. *Angew. Chem. Int. Ed.* **2017**, *56* (5), 1269–1272.
- (4) Frey, L.; Lakomek, N.-A.; Riek, R.; Bibow, S. *Angew. Chem. Int. Ed.* **2017**, *56* (1), 380–383.
- (5) Zeppelin, T.; Ladefoged, L. K.; Sinning, S.; Periole, X.; Schiøtt, B. *PLOS Comput. Biol.* **2018**, *14* (1), e1005907.
- (6) Nyholm, T. K. M.; Özdirekcan, S.; Killian, J. A. *Biochemistry (Mosc.)* **2007**, *46* (6), 1457–1465.
- (7) Vargas, C.; Cuevas Arenas, R.; Frotscher, E.; Keller, S. *Nanoscale* **2015**, *7* (48), 20685–20696.
- (8) Imura, T.; Tsukui, Y.; Taira, T.; Aburai, K.; Sakai, K.; Sakai, H.; Abe, M.; Kitamoto, D. *Langmuir* **2014**, *30* (16), 4752–4759.
- (9) Banerjee, S.; Huber, T.; Sakmar, T. P. *J. Mol. Biol.* **2008**, *377* (4), 1067–1081.
- (10) Bayburt, T. H.; Leitz, A. J.; Xie, G.; Oprian, D. D.; Sligar, S. G. *J. Biol. Chem.* **2007**, *282* (20), 14875–14881.
- (11) Rico, C. A.; Sakmar, T. P.; Huber, T. *Biophys. J.* **2014**, *106* (2), 104a–105a.
- (12) Raschle, T.; Lin, C.; Jungmann, R.; Shih, W. M.; Wagner, G. *ACS Chem. Biol.* **2015**, *10* (11), 2448–2454.
- (13) Phillips, M. C. *J. Lipid Res.* **2013**, *54* (8), 2034–2048.

- (14) Nasr, M. L.; Baptista, D.; Strauss, M.; Sun, Z.-Y. J.; Grigoriu, S.; Huser, S.; Plückthun, A.; Hagn, F.; Walz, T.; Hogle, J. M.; et al. *Nat. Methods* **2017**, *14* (1), 49–52.
- (15) Seeman, N. C.; Sleiman, H. F. *Nat. Rev. Mater.* **2018**, *3* (1), 17068.
- (16) Rothmund, P. W. K. *Nature* **2006**, *440* (7082), 297–302.
- (17) Douglas, S. M.; Dietz, H.; Liedl, T.; Högberg, B.; Graf, F.; Shih, W. M. *Nature* **2009**, *459* (7245), 414–418.
- (18) Hong, F.; Zhang, F.; Liu, Y.; Yan, H. *Chem. Rev.* **2017**, *117* (20), 12584–12640.
- (19) Goodman, R. P.; Schaap, I. a. T.; Tardin, C. F.; Erben, C. M.; Berry, R. M.; Schmidt, C. F.; Turberfield, A. J. *Science* **2005**, *310* (5754), 1661–1665.
- (20) Veetil, A. T.; Chakraborty, K.; Xiao, K.; Minter, M. R.; Sisodia, S. S.; Krishnan, Y. *Nat. Nanotechnol.* **2017**, *12* (12), 1183–1189.
- (21) Schmidt, T. L.; Heckel, A. *Small* **2009**, *5* (13), 1517–1520.
- (22) Ackermann, D.; Schmidt, T. L.; Hannam, J. S.; Purohit, C. S.; Heckel, A.; Famulok, M. *Nat. Nanotechnol.* **2010**, *5* (6), 436–442.
- (23) Gonçalves, D. P. N.; Schmidt, T. L.; Koepfel, M. B.; Heckel, A. *Small* **2010**, *6* (12), 1347–1352.
- (24) Schmidt, T. L.; Heckel, A. *Nano Lett.* **2011**, *11* (4), 1739–1742.
- (25) Lu, C.-H.; Cecconello, A.; Qi, X.-J.; Wu, N.; Jester, S.-S.; Famulok, M.; Matthies, M.; Schmidt, T.-L.; Willner, I. *Nano Lett.* **2015**, *15* (10), 7133–7137.
- (26) Gür, F. N.; Schwarz, F. W.; Ye, J.; Diez, S.; Schmidt, T. L. *ACS Nano* **2016**, *10* (5), 5374–5382.
- (27) Langecker, M.; Arnaut, V.; List, J.; Simmel, F. C. *Acc. Chem. Res.* **2014**, *47* (6), 1807–1815.

- (28) Langecker, M.; Arnaut, V.; Martin, T. G.; List, J.; Renner, S.; Mayer, M.; Dietz, H.; Simmel, F. C. *Science* **2012**, *338* (6109), 932–936.
- (29) Czogalla, A.; Kauert, D. J.; Franquelim, H. G.; Uzunova, V.; Zhang, Y.; Seidel, R.; Schwille, P. *Angew. Chem. Int. Ed.* **2015**, *54* (22), 6501–6505.
- (30) Perrault, S. D.; Shih, W. M. *ACS Nano* **2014**, *8* (5), 5132–5140.
- (31) Yang, Y.; Wang, J.; Shigematsu, H.; Xu, W.; Shih, W. M.; Rothman, J. E.; Lin, C. *Nat. Chem.* **2016**, *8* (5), 476–483.
- (32) Zhang, Z.; Yang, Y.; Pincet, F.; C. Llaguno, M.; Lin, C. *Nat. Chem.* **2017**, *9* (7), 653–659.
- (33) Hagerman, P. J. *Nature* **1986**, *321* (6068), 449–450.
- (34) MacDonald, D.; Herbert, K.; Zhang, X.; Polgruto, T.; Lu, P. *J. Mol. Biol.* **2001**, *306* (5), 1081–1098.
- (35) Gish, G.; Eckstein, F. *Science* **1988**, *240* (4858), 1520–1522.
- (36) Koo, H.-S.; Wu, H.-M.; Crothers, D. M. *Nature* **1986**, *320* (6062), 501–506.
- (37) Parasassi, T.; De Stasio, G.; Ravagnan, G.; Rusch, R. M.; Gratton, E. *Biophys. J.* **1991**, *60* (1), 179–189.
- (38) Koynova, R.; Caffrey, M. *Biochim. Biophys. Acta BBA - Rev. Biomembr.* **1998**, *1376* (1), 91–145.
- (39) Denisov, I. G.; McLean, M. A.; Shaw, A. W.; Grinkova, Y. V.; Sligar, S. G. *J. Phys. Chem. B* **2005**, *109* (32), 15580–15588.
- (40) Marrink, S. J.; Risselada, H. J.; Yefimov, S.; Tieleman, D. P.; de Vries, A. H. *J. Phys. Chem. B* **2007**, *111* (27), 7812–7824.
- (41) Uusitalo, J. J.; Ingólfsson, H. I.; Akhshi, P.; Tieleman, D. P.; Marrink, S. J. *J. Chem. Theory Comput.* **2015**, *11* (8), 3932–3945.



